Catal Lett (2013) 143:333–338
DOI 10.1007/s10562-013-0971-0

Selectively Obtaining ε-Caprolactam from Cyclohexanone Oxime Over Al-MCM-41 Catalysts

Eliana G. Vaschetto · Julio D. Fernández · Sandra G. Casuscelli · Griselda A. Eimer

Received: 4 December 2012 / Accepted: 29 January 2013 / Published online: 9 February 2013

Abstract Catalysts with Al-MCM-41 structure were prepared by direct hydrothermal synthesis. Nest silanols with weakly acid character, associated to the presence of framework Al, have been identified. These silanols seem be the active sites for the rearrangement of cyclohexanone oxime. Selectivity to caprolactam of 100 % was obtained.

Keywords Al-MCM-41 · Beckmann rearrangement · ε-Caprolactam · Silanol nests · Acidity

1 Introduction

The classical process for the commercial production of ε-caprolactam involves the cyclohexanone oximation and the liquid phase Beckmann rearrangement route, which is highly selective but ecologically and economically questionable. This process has several disadvantages such as the production of large amounts of low value ammonium sulfate as a waste and the corrosion and environmental pollution caused by the use of concentrated sulphuric acid as a homogeneous catalyst [1–3]. Recently, Ichihashi [4] and Sato and co-workers [5] have developed a new process for the vapor-phase Beckmann rearrangement of cyclohexanone oxime (CHO) using a silica zeolite which has made possible the industrial production of caprolactam without producing any ammonium sulfate. Anyway, research on this field continues to be intense and, among the solid catalysts investigated, the Al-MCM-41 materials appear as very interesting. Many studies have explored the relationship between the selectivity for ε-caprolactam and the acidity. Some of them [6, 7] claim that the formation of ε-caprolactam is mainly favored by moderate acid centers present on Al-MCM-41 in their H-forms, which deeply dependent of the framework aluminum content. Meanwhile other researchers have noticed that only weak or even extremely weak acid sites, such as hydrogen bonded hydroxyls at framework defect sites (vicinal silanol groups or silanol nests), can be effective for the Beckmann rearrangement [2, 8–10] while strong acid sites accelerate the formation of by-products [11, 12]. Hence, more research is even necessary to elucidate the nature and acid strength of the active sites required for the vapor-phase Beckmann rearrangement of the CHO to obtain ε-caprolactam. In this paper, we develop and characterize Al-MCM-41 catalysts, in order to relate the incorporation degree of the aluminum into framework and the acidity (nature and strength of acid sites) with their catalytic performance in the vapor-phase Beckmann rearrangement of the CHO.

E. G. Vaschetto · J. D. Fernández · S. G. Casuscelli · G. A. Eimer (✉)
CITeQ, Facultad Regional Córdoba, Universidad Tecnológica Nacional, Maestro López esq. Cruz Roja Argentina, (5016) Córdoba, Argentina
e-mail: geimer@scdt.frc.utn.edu.ar

E. G. Vaschetto · S. G. Casuscelli · G. A. Eimer
CONICET, Córdoba, Argentina

2 Experimental

2.1 Synthesis

In a typical synthesis, cetyltrimethylammonium bromide (CTABr) was dissolved in H_2O–NaOH solution and after heating (35–40 °C) to dissolve the surfactant, the tetraethoxysilane (TEOS) was added and stirred for 30 min. After the sodium aluminate addition, the synthesis gel (molar composition: NaOH/Si = 0.50, CTABr/Si = 0.12,

$H_2O/Si = 132$ and $Si/Al = 20$ and 60) was stirred at room temperature for 7 h and hydrothermal treated at 100 °C for 6 days. To remove the template, the samples were heated under N_2 flow up to 500 °C for 6 h and then calcined at 500 °C under air flow. These were named as Al-M(x), where "x" is the Si/Al initial molar ratio. For comparison, an analogous aluminum-free MCM-41 sample was synthesized and named as Si-M.

2.2 Characterization

The X-ray diffraction (XRD) patterns were recorded in air at room temperature on a Philips PW 3830 diffractometer with Cu Kα radiation ($\lambda = 1.5418$ Å) in the range of 2θ from 1.5 to 7°.

The Al content was determined by inductively coupled plasma optical emission spectroscopy (ICP-OES), using a VISTA-MPC CCD simultaneous ICP-OES-VARIAN.

The solid state nuclear magnetic resonance (NMR) spectra were conducted on a Bruker Avance II 300 spectrometer operating at 78.2 MHz for ^{27}Al. The sample was spun at the magic angle at a rate of 5 kHZ. Experiments were carried out at ambient probe temperature. The ^{27}Al spectrum was recorded using direct polarization with pulses of 1 μs duration and a relaxation delay of 2 s. Aluminium chemical shifts are quoted with respect to 1 M aluminium nitrate solution.

Infrared analysis of the samples was recorded on a JASCO 5300 FT-IR spectrometer. In addition, in order to evaluate the strength and type of acid sites, FT-IR spectral measurements of pyridine adsorption on the samples were performed. Afterwards the background spectrum was recorded, the solid wafer was exposed to pyridine vapors until saturate the system to 46 mm Hg at room temperature. After an IR spectrum of the adsorbed pyridine at room temperature was recorded, the subsequent IR spectra were obtained following the pyridine desorption by evacuation for 1 h at 25, 50, 100 and 200 °C.

2.3 Catalytic Reactions

The catalytic reactions were carried out in a down flow fixed bed tubular glass reactor (i.d. = 8 mm and 35 cm length) at atmospheric pressure using 0.2 g of the catalyst. The reactor was placed inside a temperature controlled furnace (320 °C). A solution of 10 wt% CHO in 1-hexanol was fed using a syringe pump (5.6 ml/min). The contact time was W/F = 40 gh/mol (weight of catalyst over the feed rate). Nitrogen was used as the carrier gas (30 ml/min). The reaction products and unconsumed reactants were condensed and collected in a properly designed system in order to minimize the loss of organic vapors. In addition, under steady state, we do not observed an apparent net accumulation or depletion of mass in the system, that is, the total mass entering the system (total mass at start) was practically equal to the total mass leaving system (total final mass). The samples were analyzed using a Perkin Elmer gas chromatograph (Clarus 500) with a capillary column and a flame ionization detector (FID). The product identification was done by GC–MS Perkin Elmer (Clarus 560S).

3 Results and Discussion

Table 1 summarizes the physicochemical properties of the samples prepared in this study and Fig. 1 shows their corresponding XRD patterns. The patterns XRD exhibit a main (100) reflection peak and weak two ascribed to (110) and (200) reflections, which is typical of highly ordered MCM-41 structures and consistent with the high surface area values obtained (above 1000 m^2/g).

^{27}Al NMR measurements were conducted to distinguish between tetrahedral and octahedral aluminum coordination in order to establish the degree of aluminium substitution (tetrahedral sites) in the silica framework. The spectra for our samples (Al-M(20) and Al-M(60)), shown in Fig. 2, exhibit a peak at 59 ± 2 ppm corresponding to tetrahedral coordinated aluminum into the framework and a peak at 0 ± 2 ppm attributed to the octahedral coordinated extra framework aluminum [13–16]. The wt% of tetrahedral Al in the samples (Al_{Td} wt%) was determined from the Al_{Td} % (calculated from the integrated intensity of the NMR peak at 59 ± 2 ppm) multiplied with the overall Al content (Al wt%) (Table 1). Then, it is possible to observe a larger incorporation and stabilization of Al into the framework for the sample with the higher Al content (Si/Al ratio = 20). In addition, the infrared spectra in the 400–1600 cm^{-1} range for the KBr-pelletized samples are shown in Fig. 2. The main bands described in the literature for MCM-41 are found in our samples [13, 14, 17, 18]. Moreover, a band clearly visible at 960 cm^{-1} [3, 19–21] can be interpreted in terms of the overlapping of both Si–OH groups and Si–O–Al bonds vibrations. Nevertheless, the increase in the integrated absorbance of this band when the Al content increases (shown in Table 1) can be considered as a further evidence of the heteroatom incorporation into the framework. This fact is according to the NMR results.

In order to detect the presence of silanol groups on the surface, Fig. 3 depicts the FT-IR spectra of the samples in the hydroxyl range. Before measurements, self-supported wafers of the samples were degassed at 400 °C for 7 h. It is known that there can be several types of surface silanol groups with different acidic properties: terminal, geminal, vicinal and nests [4, 5, 22–26]. All our spectra exhibited a

Table 1 Physico-chemical properties, IR and NMR data of the synthesized solids

Sample	Si/Al[a] (initial molar ratio)	a_0^b (nm)	Area (m^2/g)	Al[c] (wt%)	Al_{Td} (%)[d]	Al_{Td} (wt%)	A^e_{960} (cm^{-1})	A^f_{1632} (cm^{-1})
Al-M(20)	20	4.45	1242	1.65	19.35	0.3192	1.1	1.35
Al-M(60)	60	4.45	1277	0.42	18.03	0.0757	0.7	0.91
Si-M	–	4.20	1182	–	–	–	0.3	0.13

[a] In the synthesis gel

[b] $a_0 = (2/\sqrt{3})\ d_{100}$

[c] By ICP-OES

[d] By NMR data

[e] Integrated absorbance (cm^{-1}) of 960 cm^{-1} IR band

[f] Integrated absorbance (cm^{-1}) of 1632 cm^{-1} IR band after pyridine adsorption

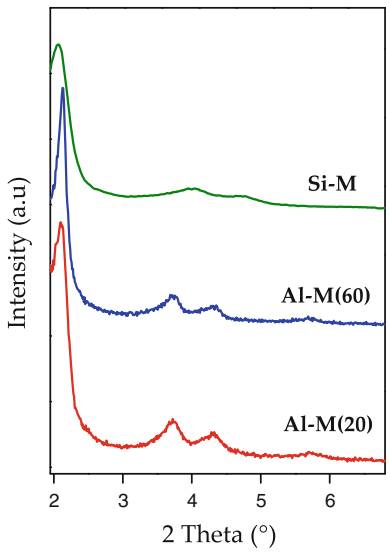

Fig. 1 XRD patterns of the synthesized samples

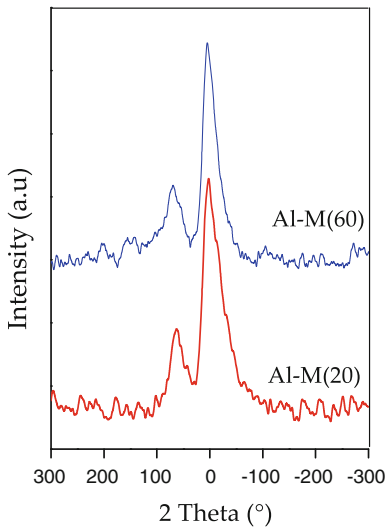

Fig. 2 ^{27}Al solid state MAS NMR spectra of the samples Al-M(20) and Al-M(60)

broad and intense band, attributed to hydrogen bonded hydroxyl groups [22–25], that could be deconvoluted into two contributions at about 3700 and 3590–3600 cm^{-1}. According to the literature [4, 5, 22, 23] these two contributions have been assigned to vicinal silanol groups and silanol nests, respectively, generated at framework defect sites probably due to the method used for catalyst preparation. It is possible observe that even if the siliceous MCM-41 contains silanol nests, its relative proportion increases with increasing framework aluminum amount, according the Al content increases (see Fig. 4; Table 1). The higher acidic character of the nest silanol is consistent with its lower vibrational frequency (3600 cm^{-1}) in the FT-IR spectrum (lower O–H bond strength) and contrasts with higher frequencies for vicinal silanols (3700 cm^{-1}) observed in our samples. Moreover, for our samples, the component assigned to nest silanol slightly shifts to a lower frequency (3590 cm^{-1}) in the Al modified samples compared with the siliceous sample. This evidences a weakening of O–H bond and hence an enhanced acid character of the nest silanols as result of the incorporation of aluminum. Finally, it is notable that no bands corresponding to Brønsted acid sites, arising from isolated bridging Si(OH)Al hydroxyl groups, were found in this region of IR spectrum [24–26].

The chemisorption of pyridine followed by IR studies is usually a useful probe to detect the presence and nature of acid sites on a catalyst [27]. Figure 5 show the FT-IR spectra of the samples recorded after the adsorption of pyridine at room temperature and subsequent evacuation at 25, 50, 100 and 200 °C. All our samples show bands at 1597 and 1447 cm^{-1} assigned to pyridine bonded to silanol groups whose hydroxyls are not capable to protonate pyridine [3, 24, 25, 27–30]. However, some contribution (overlapping these bands) from pyridine bonded to Lewis acid sites on the Al-M samples, due mainly to the presence of extra-framework aluminum oxide, could be considered [3, 24, 25, 27, 28, 31, 32]. Thus, the fact that, upon

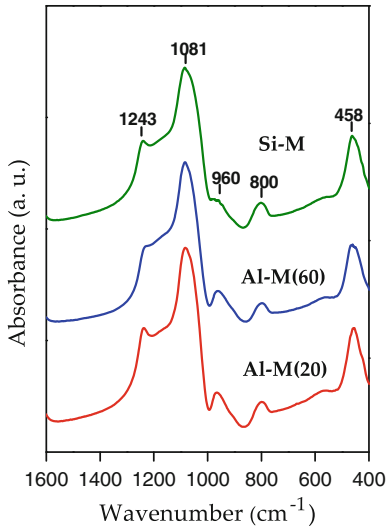

Fig. 3 FT-IR spectra of the synthesized samples in the 400–1600 cm^{-1} range

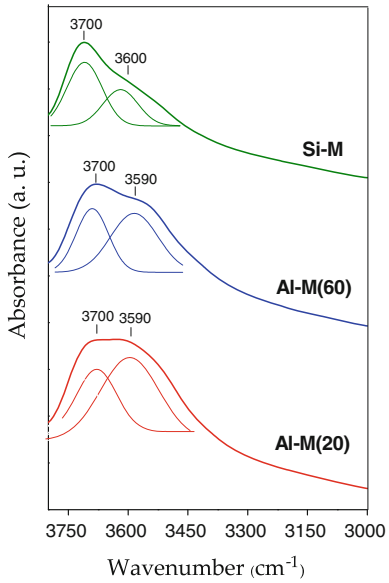

Fig. 4 FTIR spectra of the synthesized samples in the hydroxyl stretching region, after degassing at 400 °C

evacuation at 100 °C, the integrated absorbance of the bands at 1597 and 1447 cm^{-1} is slightly higher for the Al-M samples than for the purely siliceous material would be giving account for these Lewis sites capable to retain the pyridine until 100 °C. On the other hand, the presence of a band at 1632 cm^{-1}, which is remarkably more intense for the Al-M samples, can be attributed to pyridine interacting with acid hydroxyls [26, 32, 33]. In this sense, Sato and co-workers [5] investigated the acidity of different silanol species and found that the nest silanol's acidity is the strongest of all silanols; thus the nest silanols can give a proton to a basic molecule easier than other silanols because their deprotonated species might be stabilized with the help of hydrogen bonding [4, 5]. This allows us to postulate that the OH groups associated with the 3590 cm^{-1} band (nest silanols) could be mainly involved in pyridine protonation on our Al-M samples [33]. Under evacuation at 50 °C the band at 1632 cm^{-1} tends to disappear, indicating that these Brønsted sites are of a very weak character. Taking into account that all of the measurements were affected by the wafer weight, the integrated absorbances (A_{1632}) of the 1632 cm^{-1} IR band (acid silanols) after pyridine absorption at room temperature, have been calculated to estimate the acid site density (Table 1). It is noteworthy that although the siliceous sample possesses silanol nests, its acid silanol density is very low. Thus, this acidity arising from silanols can be clearly associated with the higher proportion of framework Al, according to the Al content increases. The results confirm that the introduction of Al into the mesoporous framework not only increases the proportion of silanol nests but also enhances their acid strength, likely due to an inductive effect of the heteroatom present.

Table 2 shows the catalytic results for the vapor-phase Beckmann rearrangement of the CHO in function of time on stream (TOS) over the synthesized catalysts at 320 °C and W/F = 40 gh/mol. The ε-caprolactam selectivity was 100 % during 48 h over the three catalysts. Meanwhile, the conversion initially decreased during the first hour of reaction and then, under steady state, remained practically constant. Moreover, to control the catalyst at the end of the reaction, it was recovered, heated at 500 °C in air and weighed. A negligible difference in the mass was determined. Therefore, it is suggested that the presence of non volatile species adsorbed on catalyst surface, which could poison the active sites, is insignificant. On the other hand, the conversion values for the different catalysts decrease in the order Al-M(20), Al-M(60) and Si-M. Considering that Si-M presents a negligible activity and that strong acid sites can accelerate the formation of by-products [11, 12], we propose that the weakly acid nest silanols, related with the presence of framework Al, are the most favorable sites for catalyse this reaction [4, 5, 23]. These acid hydroxyl groups seem to have a suitable acid strength to give a proton to CHO, playing an important role in the Beckmann rearrangement of the CHO towards ε-caprolactam. Thus, the results indicate that such weak acid sites increasing with the Al content, lead to an enhanced catalytic activity for the Al-M(20) sample.

Concluding, we have attempted to understand, here, the active site nature involved in the Beckmann rearrangement using mild conditions, but an optimization of the reaction conditions is necessary in order to increase the yield to ε-caprolactam.

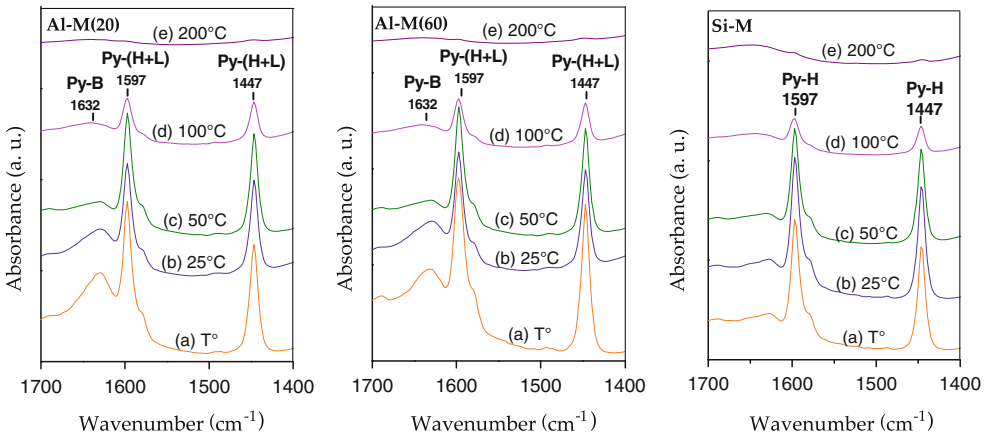

Fig. 5 FT-IR of pyridine adsorbed on the samples at *a* room temperature and after subsequent evacuation at *b* 25, *c* 50, *d* 100 and *e* 200 °C

Table 2 Conversion of CHO in the Beckmann rearrangement over the synthesized catalysts

TOS (h)	Conversion (% mol)		
	Si-M	Al-M(20)	Al-M(60)
0.25	3.7	60.43	30.91
0.50	2.1	49.23	21.24
1.00	1.5	38.56	16.08
2.00	1.4	37.52	13.12
3.00	1.3	37.48	12.23
4.00	1.3	37.45	11.91
5.00	1.3	37.31	11.50
6.00	1.2	36.82	11.03
12.00	1.2	36.80	11.00
24.00	1.2	36.80	11.00
36.00	1.2	36.79	11.00
48.00	1.2	36.79	11.00

Reaction conditions temperature = 320 °C; W/F = 40 gh/mol; CHO/1-hexanol = 1:9 wt%; N_2 = 30 ml/min

4 Conclusions

Al modified MCM-41 mesoporous molecular sieves have been prepared by a direct synthesis method. The NMR and FT-IR results demonstrate that a higher Al content favors the higher incorporation of Al into the framework. The used synthesis procedure leads to the formation of silanol nests at framework defect sites, whose density and acid character enhance when Al is introduced into the framework. Thus, studies of adsorption and thermodesorption of pyridine followed by FT-IR allow us to identify a very weak Brønsted acidity associated with these nest silanols on Al-MCM-41 materials. Meanwhile, evidences of Lewis acidity can be related, at least mainly, to the presence of extra-framework aluminum oxide species.

Rearrangement of CHO was carried out on Al-MCM-41 with selectivity to ε-caprolactam of 100 %. Under the mild reaction conditions employed (320 °C and W/F = 40 gh/mol), the Al-M(20) sample showed the highest yield to ε-caprolactam during 48 h of stream, exhibiting also resistance to poisoning. The nest silanols with very weak Brønsted acidity seem to be the most favorable sites for catalyze the Beckmann rearrangement of the CHO towards ε-caprolactam. Since Si-MCM-41 material presents a negligible activity, we suggest that the introduction of Al in our materials plays a key role for the performance of the active sites.

Acknowledgments CONICET Researchers: S.G.C. and G.A.E. CONICET Fellowship: E.G.V. The authors are grateful to CONICET and UTN-FRC for the financial support.

References

1. Ngamcharussrivichai C, Wu P, Tatsumi T (2007) Catal Commun 8:135
2. Conesa T, Campelo J, Luna D, Marinas J, Romero A (2007) Appl Catal B 70:567
3. Conesa T, Hidalgo J, Luque R, Campelo J, Romero A (2006) Appl Catal A 299:224
4. Ichihashi H (2002) Series studies in surface science and catalysis. Catal Sci Technol 145:73
5. Izumi Y, Ichihashi H, Shimazu Y, Kitamura M, Sato H (2007) Bull Chem Soc 7:1280
6. Chaudhari K, Bal R, Chandwadkar A, Sivasanker S (2002) J Mol Catal A 177:247
7. Forni L, Tosi C, Fornasari G, Trifiro F, Vaccari A, Nagy J (2004) J Mol Catal A 221:97
8. Singh P, Bandyopadhyay R, Hegde S, Rao B (1996) Appl Catal A 136:249
9. Herrero E, Anunziata O, Pierella L, Orio O (1994) Lat Am Appl Res 24:195
10. O'Sullivan P, Forni L, Hadnett B (2001) Ind Eng Chem Res 40:1471
11. Sato H, Hasabe S, Sakurai H, Urabe K, Izumi Y (1987) Appl Catal 29:107
12. Ushikubo T, Wada K (1994) J Catal 148:138
13. Eimer G, Pierella L, Monti G, Anunziata O (2002) Catal Lett 78:65
14. Eimer G, Pierella L, Monti G, Anunziata O (2003) Catal Commun 4:118
15. Ko A, Hung C, Chen C, Ouyang K (2001) Catal Lett 71:219
16. Chang J, Ko A (2004) Catal Today 97:241

17. Eimer G, Casuscelli S, Ghione G, Crivello M, Herrero E (2006) Appl Catal A 298:232
18. Palani A, Gokulakrishnan N, Palanichamy M, Pandurangan A (2006) Appl Catal A 304:152
19. Mao D, Lu G, Chen Q (2005) Appl Catal A 279:145
20. Cedeño L, Hernandez D, Klimova T, Ramirez J (2003) Appl Catal A 241:39
21. Corma A (1997) Chem Rev 97:2373
22. Heitmann G, Dahlhoff G, Hölderich W (1999) Appl Catal A 185:99
23. Hölderich W, Röseler J, Heitmann G, Liebens A (1997) Catal Today 37:353
24. Jentys A, Kleestorfer K, Vinek H (1999) Microporous Mesoporous Mater 27:321
25. Chakraborty B, Viswanathan B (1999) Catal Today 49:253
26. Zholobenko V, Plant D, Evans A, Holmes S (2001) Microporous Mesoporous Mater 44:793
27. Chanquía C, Andrini L, Fernández J, Crivello M, Requejo F, Herrero E, Eimer G (2010) J Phys Chem C 114:12221
28. Eimer G, Casuscelli S, Chanquia C, Elías V, Crivello M, Herrero E (2008) Catal Today 133:639
29. Trong On D, Nguyen S, Hulea V, Dumitriu E, Kaliaguine S (2003) Microporous Mesoporous Mater 57:169
30. Srinivas D, Srivastava R, Ratnasamy P (2004) Catal Today 96:127
31. Mokaya R, Jones W, Luan Z, Alba M, Klinowski M (1996) Catal Lett 37:113
32. Otero Arean C, Rodriguez Delgado M, Montouillout V, Lavalley J, Fernandez C, Cuart Pascual J, Parra L (2004) Microporous Mesoporous Mater 67:259
33. Escalona Platero E, Peñarroya Mentruit M, Otero Arean C, Zecchina A (1996) J Catal 162:268